PHYSICAL REVIEW B VOLUME 23, NUMBER 4 15 FEBRUARY 1981

Short-range order in theoretical models of binary metallic glass alloys

D. S. Boudreaux
Allied Chemical Corporation, Corporate Research Center, Morristown, New Jersey 07960

H. J. Frost
Department of Engineering and Applied Science, Harvard University, Cambridge, Massachussets 02139
(Received 8 September 1980)

Computer-generated models of metallic glass alloys are explored to exhibit the short-range order of their atomic structure. Binary alloys Pd-Si, Fe-P, and Fe-B are studied as a function of composition. Several approaches are used. The distribution of near-neighbor types is calculated in detail, from which it is argued that a specific coordination is preferred and satisfied by a local unit structure around each metalloid. The metalloids are removed from the structure and the size distribution and shapes of the Bernal holes remaining are calculated; the results corroborate the conclusion drawn above. The local geometry is explored by computer graphic methods and a surprising degree of regularity is discovered. Two local geometries dominate the surroundings of metalloid species: the octahedron and the trigonal prism. The relative occurrence of each is seen to vary with composition but the two methods used differ as to the degree of variation. Finally, the alloy density is calculated from a Voronoi polyhedral analysis for the first time. Density and its variation with composition are seen to be adequately simulated by the models under study.

I. INTRODUCTION

Recently a number of computer-generated models of metallic glass alloys of the transition metal-metalloid type have been described[1]; they possess many of the measured characteristics of such materials. One of the more striking features of these models is the fact that each metalloid has a constant number of metal near neighbors even as the composition of the alloy is changed. It was suggested that the metalloid sites form the center of some kind of molecular unit which is characteristic of the alloy system. The existence of such units has been proposed by the independent arguments of Gilman.[2] Taking the unit concept literally, Gaskell[3] has built and analyzed some small but successful model structures. We have sought to clarify the nature of the short-range distribution of atoms in models of metallic glass so as to shed further light on the kind of order which might be responsible for the deductions made earlier strictly on the basis of statistical measurements.

Three approaches are reported in this paper. First we calculated the distribution of near neighbors in more detail by actually studying the neighbors of each atom individually. Secondly we used computer graphic techniques to produce pictures of the local geometry. Finally, a new kind of analysis was applied to tabulate the distribution of Bernal hole[4] sizes in the models with and without metalloid atoms included.

Density is one of the simplest physical quantities one can measure, and it was realized very early[5] that in metallic glasses it was only a few percent lower than values associated with crystalline alloys of similar composition. However, the calculation of density from models is one of the most difficult tasks to accomplish with accuracy. Approximate methods were used to determine the numbers previously reported[1] but the estimates were consistently too low. In this paper we report the density as determined from a much more accurate calculation. This work is based on a Voronoi polyhedral analysis which was done on a few of our models by Finney.[6]

II. NEAR-NEIGHBOR ANALYSIS

All information on numbers of near neighbors obtained to date[1] on the computer-generated models is based on the coordination numbers deduced from calculated radial distribution functions. The coordination number was defined as the area under the first peak of a proper partial radial distribution function, i.e., the number distribution of distances of atoms of a certain type from a central atom also of a particular type. The area was determined by integrating to the first minimum beyond the first peak. This procedure lacks precision in that, for some sites, it includes more than first neighbors and, for others, it misses some atoms which are proper near neighbors. In the present case we have analyzed for the distribution of near neighbors in different and more revealing ways.

For each nonsurface atom in a structure, a search was made for neighbors within an acceptance limit. The limit is defined in terms of the hard-sphere-touching distance but adds a tolerance of a few percent to it. In practice we find that 10% is a realistic tolerance; we base this on a number of calculations for different tolerances. As we increase to 8 or 9%, the distribution of

neighbors shows pronounced changes in shape. Further changes in shape do not occur until tolerances of 12 or 13% are allowed. The neighbors are catalogued as to the number of each type found and as to the type of the central atom. Thus for each type atom, we can count the number of times it is found with a given number of neighbor types; e.g., in a binary Fe-B alloy, how many times does one find boron sites with, for example , 6 iron near neighbors?

A more meaningful measure, is however, the probability of the occurrence of a site with a given number of neighbors of each type. Table I gives this information in detail for the Pd-Si

TABLE I. Probability of the occurrence of a site with a given number of neighbors for the Pd-Si alloy series.

(a) Probability of Pd site with N(Pd) + M(Si) neighbors

	M/N	6	7	8	9	10	11	12	total
	0			0.003	0.006	0.032	0.009	0.006	0.056
	1		0.006	0.023	0.064	0.061	0.015	0.003	0.172
	2		0.017	0.108	0.157	0.076			0.358
$Pd_{75}Si_{25}$	3	0.009	0.041	0.093	0.105	0.026			0.274
	4	0.009	0.038	0.044	0.012				0.103
	5	0.003	0.012	0.012					0.027
	6		0.012						0.012
	total	0.021	0.126	0.283	0.344	0.195	0.024	0.009	1.00
	M/N	6	7	8	9	10	11	12	total
	0			0.006	0.023	0.051	0.031	0.006	0.117
	1		0.006	0.049	0.111	0.077	0.037	0.003	0.283
	2		0.023	0.063	0.160	0.069	0.009		0.324
$Pd_{80}Si_{20}$	3	0.006	0.046	0.060	0.063	0.020	0.003		0.198
	4	0.003	0.020	0.020	0.009	0.009			0.061
	5		0.017	0.003					0.020
	total	0.009	0.112	0.201	0.366	0.226	0.080	0.009	1.00
	M/N	6	7	8	9	10	11	12	total
	0		0.006	0.017	0.084	0.122	0.061	0.012	0.302
	1		0.012	0.061	0.151	0.122	0.023		0.369
	2	0.003	0.020	0.075	0.096	0.032			0.226
$Pd_{85}Si_{15}$	3		0.020	0.041	0.014	0.012			0.087
	4		0.012						0.012
	5		0.003						0.003
	total	0.003	0.073	0.194	0.345	0.288	0.084	0.012	1.00

(b) Probability of Si site with N(Pd) + M(Si) neighbors

	M/N	5	6	7	8	9	total
	0		0.028	0.165	0.220	0.018	0.431
	1	0.009	0.064	0.248	0.110		0.431
$Pd_{75}Si_{25}$	2	0.009	0.046	0.055			0.110
	3		0.028				0.028
	total	0.018	0.166	0.468	0.330	0.018	1.00
	M/N	5	6	7	8	9	total
	0	0.011	0.044	0.484	0.165	0.022	0.726
	1		0.033	0.110	0.066		0.209
$Pd_{80}Si_{20}$	2		0.011	0.033	0.011		0.055
	3		0.011				0.011
	total	0.011	0.099	0.627	0.242	0.022	1.00
	M/N	5	6	7	8	9	total
	0	0.017	0.052	0.328	0.276	0.017	0.690
$Pd_{85}Si_{15}$	1		0.086	0.121	0.069		0.276
	2			0.034			0.034
	total	0.017	0.138	0.483	0.345	0.017	1.00

alloy series. The Pd-Si system has been the basis of more studies than any other binary alloy. In addition, the same model structure used to describe Pd-Si is expected to serve as model for an alloy in the Fe-P system.[1] Table II lists the same data for the Fe-B alloy series which is an important magnetic material. The three compositions studied are below, near, and above that composition at which the glass state is most easily reached by the normal quenching process. The number in the Mth row and Nth column of the table specifies the probability of a site being found with N metal neighbors and M metalloid neighbors (neighbors defined as above). The calculations are based on a sample of approximately 500 atoms in a spherical shell whose boundaries are nearly equidistant from the model center and its outer surface. In general the trend is as expected: the more metalloid neighbors a site has, the less room for metal neighbors. One point to note in part (b) of Tables I and II is that some metalloid sites are listed as having metalloid neighbors and in a few cases more than one. The original model-building procedure attempted to

TABLE II. Probability of the occurrence of a site with a given number of neighbors for the Fe-B alloy series.

(a) Probability of Fe site with N(Fe) + M(B) neighbors

	M/N	6	7	8	9	10	11	12	total
	0				0.109	0.038	0.044	0.003	0.104
	1			0.019	0.063	0.099	0.060	0.006	0.247
	2			0.014	0.136	0.131	0.044		0.325
$Fe_{75}Be_{25}$	3		0.003	0.030	0.090	0.058	0.017		0.198
	4	0.003	0.009	0.025	0.049	0.019			0.104
	5		0.006	0.003	0.017				0.025
	6				0.003				0.003
	total	0.003	0.017	0.091	0.377	0.345	0.165	0.008	1.00
	M/N	6	7	8	9	10	11	12	total
	0		0.003	0.023	0.092	0.063	0.023		0.117
	1		0.011	0.054	0.132	0.100	0.037		0.334
	2		0.014	0.043	0.126	0.074	0.026		0.283
$Fe_{80}B_{20}$	3		0.009	0.043	0.052	0.020			0.124
	4		0.006	0.023	0.017	0.003			0.049
	5		0.003		0.003				0.006
	total		0.045	0.186	0.422	0.260	0.086		1.00
	M/N	6	7	8	9	10	11	12	total
	0			0.011	0.076	0.127	0.084	0.025	0.323
	1			0.022	0.095	0.173	0.086	0.008	0.384
	2			0.019	0.068	0.089	0.025	0.003	0.204
$Fe_{85}B_{15}$	3	0.003		0.016	0.030	0.027	0.005		0.081
	4			0.003	0.008				0.011
	total	0.003		0.071	0.277	0.416	0.200	0.036	1.00

(b) Probability of B site with N(Fe) + M(B) neighbors

	M/N	4	5	6	7	8	total
	0	0.008	0.092	0.496	0.176	0.017	0.789
$Fe_{75}B_{25}$	1		0.050	0.101	0.034		0.185
	2	0.008	0.008	0.008			0.025
	total	0.017	0.150	0.605	0.210	0.017	1.00
	M/N	4	5	6	7	8	total
$Fe_{80}B_{20}$	0		0.184	0.713	0.092	0.011	0.100
	1						0.000
	total		0.184	0.713	0.092	0.011	1.00
	M/N	4	5	6	7	8	total
$Fe_{85}B_{15}$	0		0.047	0.438	0.328	0.016	0.829
	1		0.016	0.141	0.016		0.173
	total		0.063	0.579	0.344	0.016	1.00

avoid the occurrence of near-neighbor metalloids in order to simulate the expected chemical ordering in the alloy. During the energetic relaxation of the hard-sphere model, a few near-neighbor metalloids occur at statistically insignificant levels, i.e., their contribution to the radial distribution function (RDF) is in the noise of the calculation. Within the 10% tolerance of sphere touching used in this study to find neighbors, there is a significant number of metalloid-metalloid pairs found. The more metalloid one tries to stuff into the structure (compare $Pd_{75}Si_{25}$ to $Pd_{85}Si_{15}$), the more frequent the occurrence of such pairs, as one might expect. As the tolerance is tightened, the total probability of the rows $M=0$ in Tables I(b) and II(b) exceeds 0.9. However, for all models except those with very few and very small metalloids, it is impossible to avoid some metalloid-metalloid nearest neighbors. This may also be true of real metallic glasses in which case the double metalloid sites could be very interesting, Existing experiments have not ruled out the existence of such sites occurring with the probabilities predicted here.

A graphic representation of some of these data is given in Fig. 1 for the Pd-Si series; basically the row and column totals are plotted as histograms. Figure 2 illustrates the same data summary for Fe-B alloys. In each case at least half of the metalloids occur with the dominant coordination, 6 for Fe-B and 7 for Pd-Si (or Fe-P). The most notable feature is the sharpening of the peak describing the number of metals surrounding the metalloid [Figs. 1(a) and 2(a)] near the center of the composition range, i.e., at 80/20. At this composition the geometry of the molecular units formed by a central metalloid and its metal neighbors are found in high preference with a fixed number of vertices. Further, we have been able to describe the shape of these units in the Fe-B system as described in a later Figs. 1(b) and 2(b) have been used to calculate the hyperfine field distribution in Fe-based alloys and compared to data extracted from Mössbauer experiments.[7] The peaks of these distributions shift to smaller numbers of metalloid neighbors as metalloid content is reduced. Likewise the distribution of metal-metal neighbors [Figs. 1(c) and 2(c)] sharpens as the alloy composition approaches pure metal. Both of these observations fit one's intuitive expectations.

III. SHORT-RANGE GEOMETRY

A constant coordination number, of course, does not necessarily imply that the geometric arrangements of neighbors is unique. In this section we try to explore this point. We view each of the near neighbors of a given atom as a vertex of a polyhedron. As long as there are more than four vertices, there are a number of possibilities as to the shape of the polyhedron formed.[4] We are primarily concerned with the geometry of the metal atoms surrounding the smaller metalloid atoms. In the Fe-B models most boron atoms have six iron near neighbors. The most regular shapes with six vertices are the octahedron and the trigonal prism, although several distorted shapes may be defined in between these two. For the Pd-Si models, the silicon atoms most frequently occur with seven or eight palladium near neighbors. A variety

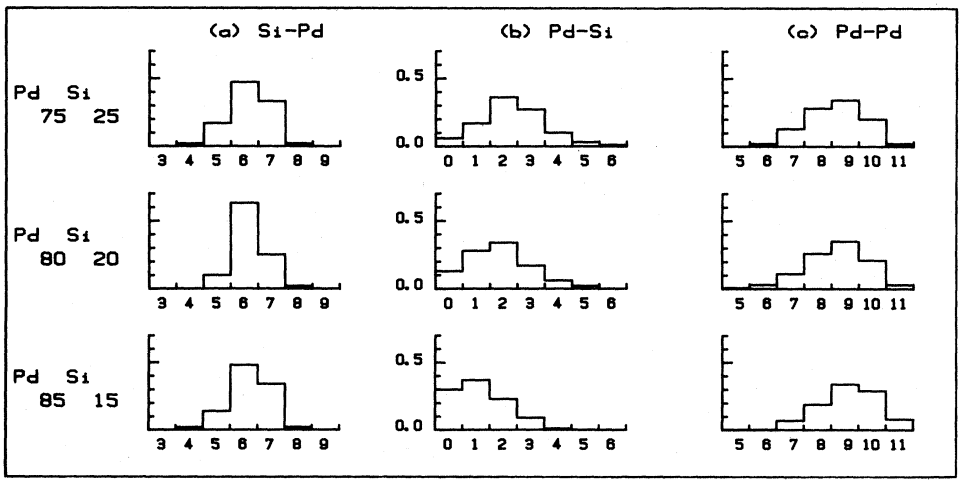

FIG. 1. Probability distribution of the number of near neighbors in models of Pd-Si glass alloys. (a) Pd atoms around Si atoms, (b) Si atoms around Pd atoms, and (c) Pd atoms around Pd atoms. Near neighbors are defined as atoms within 10% of the hard-sphere-touching distance.

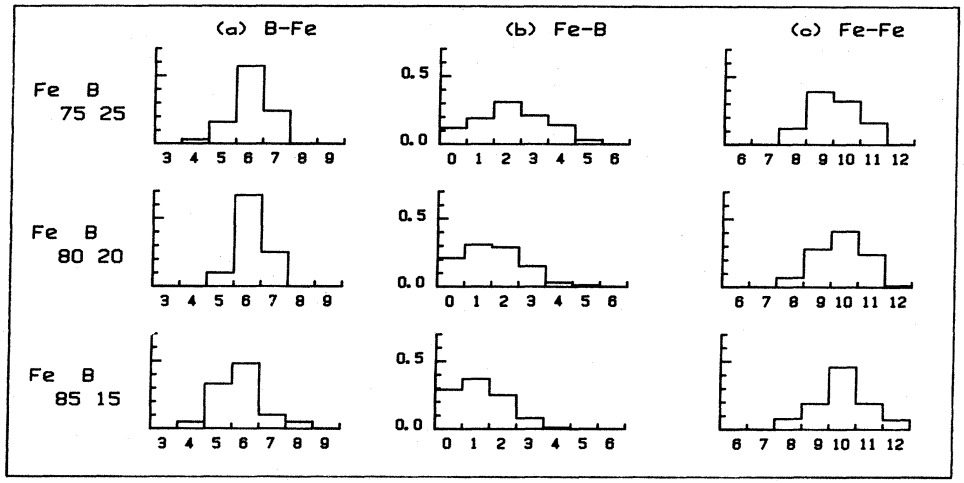

FIG. 2. Probability distribution of the number of near neighbors in models of Fe-B glass alloys. (a) Fe atoms around B atoms, (b) B atoms around Fe atoms, and (c) Fe atoms around Fe atoms. Near neighbors are defined as atoms within 10% of the hard-sphere-touching distance.

of shapes with seven or eight vertices are possible, including trigonal prisms with one or two half-octahedral caps, and the square (Archimedian) antiprism.

In the Fe-B and Pd-Si models we investigated the frequency with which the various shapes occurred by direct inspection of computer graphic displays of the atoms surrounding each metalloid. The polyhedra observed are not exactly regular but occur with varying degrees of distortion. For example, a continuous range of distortions is available between the octahedron and the trigonal prism. Thus it is necessary to establish explicit procedures which define whether a specific neighbor polyhedron is one shape or another. Two approaches have been used. (1) According to the network of near-neighbor connections between the metal atoms forming the shape, and (2) according to the directions from the center (or metalloid) to the surrounding atoms. We have concentrated our efforts on the case of six metal atoms surrounding a metalloid, as appropriate for the Fe-B models.

For the network approach we make connections between all the metal atoms that are closer to each other than some particular distance. The shape is then defined according to the topology of the network of connections (which we may call edges) that surround the metalloid. If a larger neighbor distance is used for a particular arrangement, then there may be more connections created which would result in a change of the topology of the network; thus the identification of the shape will change. Statistics that report the frequency of occurrence of various network shapes are incomplete without explicit specification of the nearest-neighbor distance. For this purpose we have used 1.30 metal-sphere diameters. If too small a neighbor distance is used, the shapes will not be identified in a meaningful way. This is because a mildly distorted regular shape is likely to have one or another edge stretched beyond 1.1 or 1.2 diameters, while it still remains more nearly one shape than any other. At the other extreme, too large a neighbor distance will give confusing results. For example, with a neighbor distance of $\sqrt{2}$, the diagonals on the three square faces of a regular trigonal prism would become edges, and the network identification would be meaningless.

We limit the catalog of possible network shapes to those that have no "faces" with more than four edges. (These edges need not be exactly coplanar.) Shapes with five or more edges are not generally useful to describe the complete surroundings of the metalloid; the five-edged face can be considered an open gap in the coordination sphere. Such a gap often occurs when we are considering the shape formed by the metal atoms surrounding a metalloid that has another metalloid as nearest neighbor that has not been counted as part of the shape. With the limitation to three- and four-edged faces, the complete catalog of possible network shapes with five or six vertices is shown in Fig. 3. All the six vertex (point) figures except the trigonal prism can be made up of two of the five-point figures joined together at four-edged faces. All the six-point figures, including the trigonal prism, can be made by breaking some number of edges in an octahedron. For seven vertices there are many different possible networks that are topologically distinct.

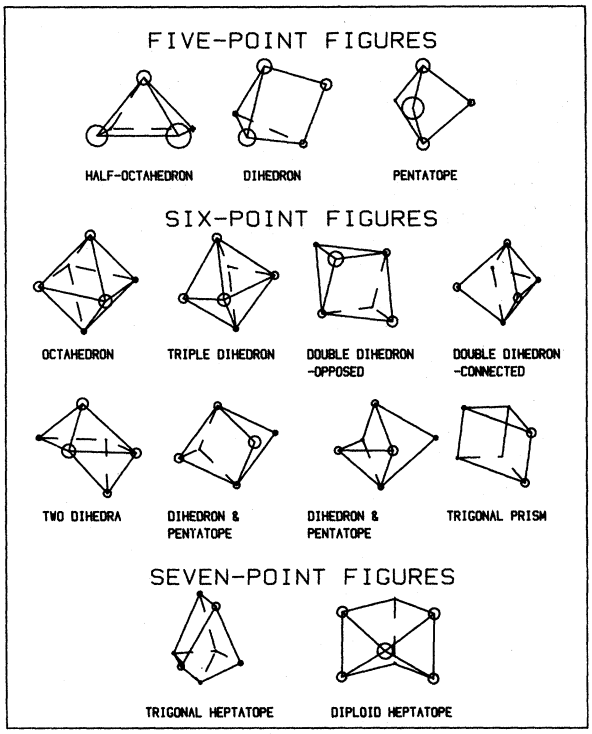

FIG. 3. Shapes used in the catalog of Table III. The five-point figures provide definitions. The octahedron is the polygon with the maximum number of edges. The sequence of six-point figures proceeds by successively breaking bonds (eliminating edges) until the trigonal prism is reached; it has three fewer bonds than the octahedron. There are two six-point figures (pentatopes) missing; they are generated by breaking four bonds but are not observed in the model structures.

Only the two shown in Fig. 3, however, cannot be made up from two or three of the five- and six-vertex figures. For eight points there are still more possible networks, most of which can be made by combining smaller shapes. Those that cannot are the square antiprism (Archimedian antiprism[4]) and the shapes created by removing one to four edges from an antiprism (For example, a cube can be created by removing four edges.)

The alternative to the network approach of polyhedron shape definition is an approach based on the directions of the vectors from the metalloid to each of the surrounding metal atoms. (We could also have used the center of mass in place of the metalloid location.) This approach only gives meaningful results if all the metal atoms are about the same distance from the center, in the present case, within the nearest-neighbor shell. The shapes possible for, for example, six points are therefore the possible distinct ways of arranging six points on the surface of a sphere. It simplifies the range of possibilities to specify that no two points (vectors) can be closer than some given distance (angle). If the closest metal-metal approach is 1.00 and the metal atoms are 0.76 from the central metalloid, the closest vectors are at 82° from each other. This is in fact the angle between vectors to the corners of a regular trigonal prism (81.786 79°). If six points form an octahedron, the vectors will be at 90°, and for the same metal-metalloid distance the metal atoms would be spaced 1.0748 diameters. The metal atoms could be thought of as being loose to move out of position to produce a range of distorted shapes. An octahedron can be created by twisting a trigonal prism along an axis through the triangular faces until one triangle is oriented 60° from the other as depicted in Fig. 4. From this we can devise a simple method to define whether a given shape is more nearly an octahedron or a trigonal prism. One could determine which set of three vectors among the six is closest together (minimum total of the three angles between them). The end points of these vectors form a *triangle*, and the other three points necessarily form a second triangle. Each triangle is projected onto a plane perpendicular to the line joining their centers (intersection points of medians). If the projected triangles are more nearly aligned, then the figure is called a trigonal prism; if more nearly staggered (rotated by 60°) then it is called an octahedron.

Results for both types of shape definition were found by studying the neighbors (as defined in Sec. II) of individual metalloid sites by computer graphics programs. Atoms are displayed on a screen at points corresponding to their (x, y) coordinates, with symbols whose size is scaled by their z coordinates (larger means closer to viewer). For the network definition, those neighboring metal atoms closer than 1.30 diameters are connected by lines, and the shape is visually identified. To make an identification according to directional definition, a program is used which rotates the set of points on the screen at the user's instruction. In practice a variant of the procedure described above proved more effective especially in dealing with nonsixfold coordinated sites. Each triangular face is considered in turn and the existence of a second triangular face nearly parallel to the first is sought. For six vertices, if the two triangles had nearly congruent xy projections the polygon was called a trigonal prism. If one triangle was "upside down" with respect to the other, the polygon was called an octahedron. For more than six vertices the procedure becomes more complex but we could almost always find one of the underlying polygonal shapes above with an edge-

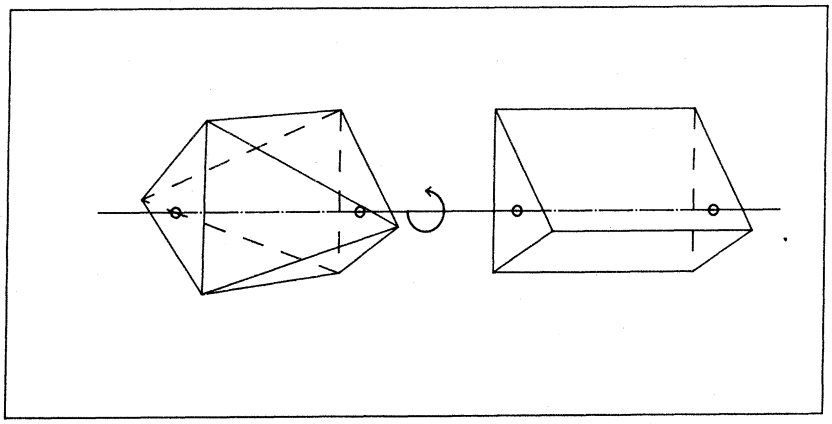

FIG. 4. An octahedron (left) can be viewed as a trigonal prism with one triangular face rotated 60° with respect to the other. The number of edges connecting the rotated triangular faces in the staggered configuration is doubled.

bridging or face-capping atom.

To minimize the number of triangular faces which had to be examined, edges were drawn only if the atoms at the vertices were within 1.10 diameters. Thus the "connections" studied by the two approaches were not exactly the same and it is clearly possible to find a given polyhedron catalogued differently, e.g., an octahedron with several edges of length l: $1.10 < l \leq 1.30$ would be recognized as an octahedron by network analysis but as some form of dihedron by direction. Moreover some of the seven-point figures could clearly be catalogued as basically octahedral by direction and trigonally prismatic by network analysis because the face caps form triangles whose plane may be nearly parallel to a distorted face of the underlying basic shape. Each approach has its advantages but unfortunately the variable "bond lengths" in the models prohibit a completely objective criterion for cataloguing short-range geometry.

An interesting trend was found in the polyhedra surrounding the boron atoms. According to the directional shape definition, most shapes in $Fe_{75}B_{25}$ were trigonal prisms. As boron content was reduced, however, we began to see a more frequent occurrence of octahedra. Typical examples of these shapes are shown in Fig. 5. The trigonal prism in Fig. 5(a) is distorted on one of its rectangular faces to allow for the almost-near-neighbor iron atom which caps the face. The interatomic forces under which these structures were produced were twice as strong between iron and boron than between iron and iron, and clearly favors the capping of the prism and in some cases distortion of a face to allow a closer proximity of the capping iron to the attractive boron site. Figure 5(b) shows an octahedrally coordinated boron site from $Fe_{85}B_{15}$. The reason for the more common occurrence of octahedra when less boron is present is clearly due to packing optimization, but we have not yet

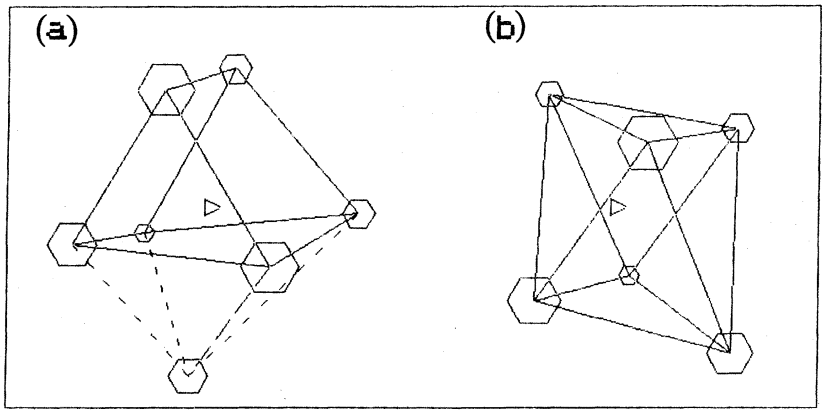

FIG. 5. Geometry of short-range order around B sites in Fe-B glass alloys. The boron is at the center of the structure shown by a triangle. The surrounding iron atoms are smaller if farther away from the viewer. (a) Trigonal prismatic coordination in $Fe_{75}B_{25}$, (b) octahedral coordination in $Fe_{85}B_{15}$.

studied the more difficult matter of packing of the polyhedra themselves as suggested by the work of Gilman[2] and of Gaskell.[3] An intuitive explanation is that the trigonal prism presents only five faces for next-nearest-neighbor iron sites, while the octahedron presents eight. In the alloys with small boron content, each boron site must accommodate more iron sites in its vicinity and this is favored by octahedral symmetry.

When the same sites were identified according to the network definitions, this trend is reversed. Results are given in Table III. Trigonal prisms are slightly more common in $Fe_{85}B_{15}$, though the difference is not large compared to the expected statistical counting errors. The conclusion must be that certain sites are identified differently by the two approaches. The various types of dihedra appear to be distorted octahedra while the two seven-point figures appear to be distorted trigonal prisms with an extra capping point. A significant number of sites are identified in Table III as "open." These are boron atoms which have a boron near neighbor; boron near neighbors were not counted as part of the surrounding network. As expected, there are more of these sites in the model with more boron.

Turning attention to the iron sites, we found that one could almost always see an icosahedral arrangement of neighbors when the coordination of neighbors was 12 [the average value, see Figs. 1 and 2, (b) and (c)]. Figure 6 shows an icosahedrally coordinate site from $Fe_{80}B_{20}$. It is shown in two views so that one can appreciate the regularity of the shape. Figure 6(a) shows the staggered pentagonal rings and the three atoms on the axis nearly aligned while Fig. 6(b) shows a 90-degree rotation to illustrate the planarity of the rings. Nucleation theory has long pointed to the inherent stability of this arrangement of atoms[8] and it has even been discussed in the context of metallic glass by Briant and Burton.[9]

TABLE III. Bernal hole shapes in Fe-B glass alloys.

	$Fe_{75}B_{25}$ [a]	$Fe_{85}B_{15}$ [a]
Half-octahedra	0.41%	0.68%
Octahedra	10.29	4.76
Dihedra	39.92	42.18
Pentatopes	0.82	0.68
Trigonal prisms	32.51	38.10
Trigonal heptatopes	2.05	3.40
Diploid heptatopes	0.0	0.68
Antiprisms	1.65	0.0
Open	12.35	8.84

[a] Edges are formed for vertices within 1.3 sphere diameters of each other.

IV. INTERSTITIAL SITES IN METAL SUBSTRUCTURE

Another related type of analysis involves finding the size of interstitial holes in the structure. Frost[4] has analyzed the hole-size distribution in two of the more well known single-size-sphere dense random-packing models. In particular we used the same approach on the binary models[1] with metalloid sites removed. The remaining model structures had large voids or holes at sites previously occupied by metalloid atoms; the size distribution of these interstitial holes is quite revealing. The site of the hole must be defined. Each of the transition-metal (TM) sites remaining in the structure is imagined to be surrounded by a unit sphere ("the atom"). Any set of four non-coplanar atom centers defines a sphere, and if no other atom centers are inside that sphere then it represents a "hole" in which a smaller sphere can be

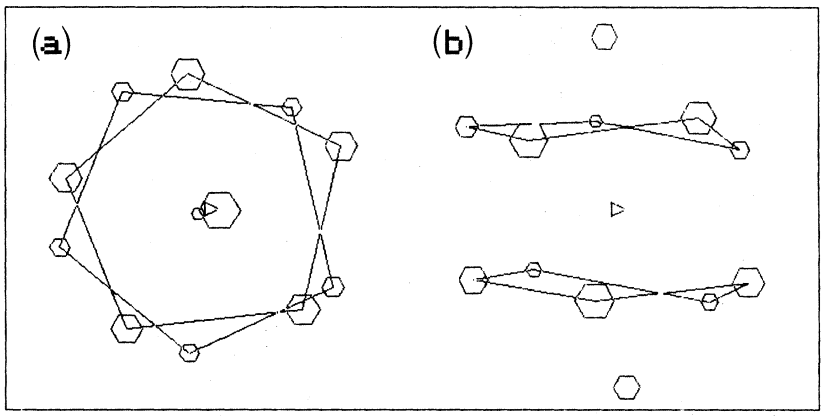

FIG. 6. Icosahedral units found around Fe (triangle) sites in Fe-B alloy models. (a) "Top view" shows staggered pentagonal rings and central line of atoms. (b) Same unit rotated 90° about the x axis show the planarity of the rings.

placed so that it touches the four original atoms and none other. The diameter of the sphere which fits in the hole is used as a measure of the hole size (units of metal atom diameters). This procedure will occasionally define overlapping small-sphere locations in a particular region, and in such cases the largest small sphere is counted and any it overlaps are discarded.

Figure 7 presents the hole-size distribution histograms of the Fe-B alloy series while Fig. 8 has the same information for alloys of $Pd_{80}Si_{20}$ and $Pd_{80}Ge_{20}$. The hole size is characterized by the diameter of an inscribed sphere in units such that the diameter of the transition metal atom is 1.0. The first peak is due to the smaller holes formed by polyhedra of metal sites as vertices but which are not big enough to enclose a metalloid. These holes exist in the original binary models before the metalloids are removed. The second peak exhibits the range of sizes of holes occupied by metalloid in the original models. The variation of hole-size distribution with changes in composition is illustrated in Fig. 7. The sizes of the holes occupied by metalloid atoms are more sharply peaked about the average size at the 80/20 composition than they are for the compositions at which the glass state is harder to form. This is consistent with sharpening of the distributions shown in Figs. 1 and 2 as discussed in Sec. II. As the size of the metalloid increases relative to the metal, e.g., Pd-Si and Pd-Ge shown in Fig. 6., the size of the hole increases accordingly and is seen as a shifting of the second peak to the right. The shape of the second peak in the dis-

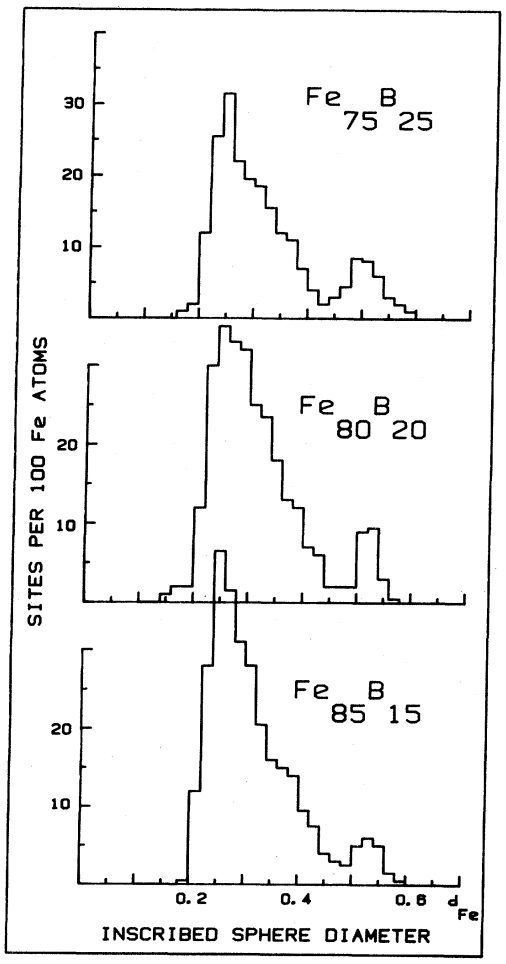

FIG. 7. Calculated hole-size distributions in Fe-B alloy models. Inscribed sphere is measured in units of Fe atom diameters. The metalloids were removed before analysis, thus the second peak is the distribution of holes which are large enough to contain boron atoms.

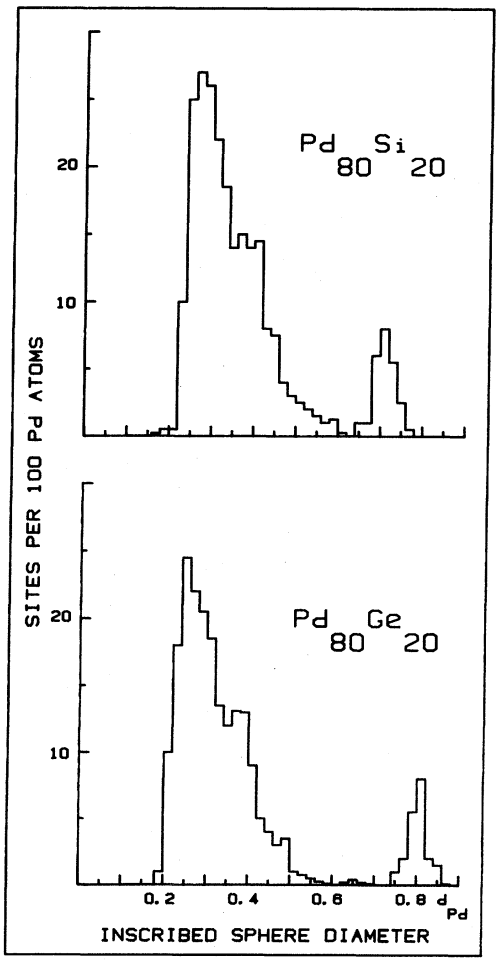

FIG. 8. Calculated hole-size distributions for Pd-based glass models. Note the large hole size for the metalloid as compared to B in Fig. 7. Also note the shoulder on the right of the first peak as discussed in the text.

tribution is seen to be sharper in the case of Pd-Ge where the metalloid is only 10% smaller than the metal. There is also a shoulder on the first peak of the distributions for the Pd glass models.

The shoulder is possibly a very interesting piece of data. It indicates two types of holes formed by metal-atom vertices and these two types could be associated with the double-potential-well concept used to explain a minimum in the temperature dependence of resistivity[10] in metallic glass alloys. This point will be the subject of further investigation, but it is also interesting to note that the first peak of the distributions for the Fe-B alloys is broader on the right side. It is known that the resistivity minimum begins to disappear as metalloid content is reduced,[11] and the sharpening of the first peak in the hole-size distribution in Fe-B alloys with decreasing amounts of boron correlates with this if the speculative association is correct.

V. MODEL DENSITY

The density of crystalline materials is very easy to calculate; one can readily determine the number and kind of atoms in a unit cell as well as the volume of that cell. The analog of the unit cell for noncrystalline materials is the Voronoi polyhedron. Each site is surrounded by a polyhedron of a specific kind and size so that the polyhedra of all sites pack together to fill space with no overlap or voids. The polyhedron is formed by the planes which perpendicularly bisect the vectors to all the near neighbors of a given site. Thus each Voronoi polyhedron contains exactly one atom, information which, with the volume, permits an exact calculation of density at a specific site. The density of the material can then be calculated from suitable averages of the local densities at the various type sites.

The procedures for performing a Voronoi polyhedral analysis are straightforward but complex Finney[6] has developed computer programs to carry out the necessary calculations and has applied them to some of the models currently being discussed, specifically the Pd-Si series with 18, 20, 22, and 25 at. % Si, respectively. These model structures are expected to serve as well for the Fe-P series of glass alloys.[1]

As a starting point, the density of the alloy $Fe_{75}P_{25}$ was determined from the polyhedral analysis on the model of that glass. This choice was made because the densities are experimentally well known and because the Fe-Fe spacing is expected to be nearly the same as it is in the crystalline material Fe_3P which is also known. The metal-metal spacing is required to determine the scaling of theoretical results to physical dimensions. Using 0.272 nm for the average Fe-Fe separation, we calculate 6.84 g/cm^3 as the density of the glass which is in respectable agreement with the measured value of 6.9 (see Fig. 9). Considering the model of the alloy $Fe_{80}P_{20}$, we find a density of 6.52 if the scaling factor is unchanged and this is in very poor agreement with experiment (point shown as inverted triangle in Fig. 9). However, a 3% shortening of the Fe-Fe spacing to 0.264 nm results in a calculated value of 7.1 g/cm^3. This change of spacing with composition was observed by Logan[12] for the Fe-P system and is numerically in accord with his measurements. The decrease in Fe atom size is consistent with a decreased amount of charge transfer from metalloid to metal as the metalloid content is reduced. However, the picture is not as simple as this. If one uses the spacings at the two compositions above to determine a linear variation of spacing with composition, and then calculates the densities at two other points (18 and 22 at. % P), the values of density are too high by 4%. The density is extraordinarily sensitive to changes in scaling since it has a cubic dependence on scale factor. Thus a good bit more detail is needed before we can resolve theory and experiment on this point.

The composition variation of density has not

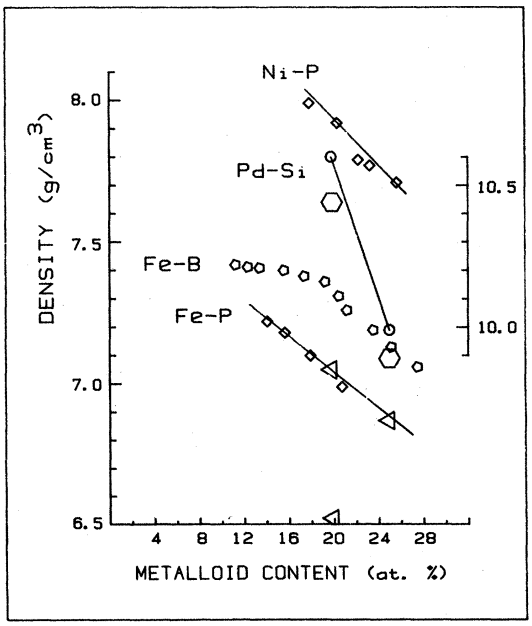

FIG. 9. Density of transition metal-metalloid glass alloys. Calculated values are given, for Pd-Si by the hexagons and for Fe-P alloys by the triangles. The scale on the right is for Pd-based alloys.

previously been reported for the Pd-Si system, but two measured values (in toluene at 22.5 °C) are given in Fig. 8. To calculate density from the models, the Pd-Pd spacing is taken from Suzuki *et al.*[13] as 0.290 nm. This results in a value of 9.88 g/cm^3 compared to the measured value of 9.98. Fukunaga *et al.*[14] report a "slight" shortening of the Pd-Pd spacing as metalloid is removed but do not quantify the amount. If we use the 3% found for Fe-Fe spacing reduction in Fe-P, the density at $Pd_{80}Si_{20}$ is calculated to be 10.4 g/cm^3 compared to a measured value of 10.63. Considering the lack of detailed understanding of the variation of metal-metal spacing with composition, one has to consider the calculated values of glass density to be in excellent agreement with measured values.

ACKNOWLEDGMENT

We gratefully acknowledge the Voronoi polyhedral analysis done by Dr. Finney on the models studied and discussion relating to the density of glass alloys. Mr. J. Wilkalis provided assistance in computer programming.

[1]D. S. Boudreaux, Phys. Rev. B 18, 4039 (1978).
[2]J. J. Gilman, Philos. Mag. B 37, 577 (1978).
[3]P. H. Gaskell, J. Non-Cryst. Solids 32, 207 (1979).
[4]H. J. Frost, Acta Metall. (in press).
[5]G. S. Cargill, III, Solid State Phys. 30, 227 (1975).
[6]J. L. Finney, unpublished.
[7]I. Vincze, D. S. Boudreaux, and M. Tegze, Phys. Rev. B 19, 4896 (1979).
[8]M. R. Hoare and P. Pal, J. Cryst. Growth 17, 77 (1972).
[9]C. Briant and J. J. Burton, Phys. Status Solidi B 85, 393 (1978).
[10]R. W. Cochrane, R. Harris, J. O. Strom-Olson, and M. J. Zuckerman, Phys. Rev. Lett. 35, 676 (1975); and P. W. Anderson, B. I. Halperin, and C. M. Varma, Philos. Mag. 25, 1 (1971).
[11]R. Hawegawa, private communication.
[12]J. Logan, Phys. Status Solidi A 32, 361 (1975); see also Ref. 14.
[13]K. Suzuki, T. Fukunaga, M. Misawa, and T. Masumoto, Mater. Sci. Eng. 23, 215 (1976).
[14]T. Fukunaga, M. Misawa, K. Fukamichi, T. Masumoto, and K. Suzuki, in *Proceedings of the 3rd International Conference on Rapidly Quenched Metals*, edited by B. Cantor (The Metals Society, London, 1978), Vol. II, p. 325.